ID-1106

STRESS ANALYSIS OF BONDED CURVED JOINTS WITH NON-UNIFROM ADHESIVE THICKNESS

Liyong Tong* and Xiannian Sun
School of Aerospace, Mechanical and Mechatronic Engineering
The University of Sydney, NSW 2006 AUSTRALIA

SUMMARY: This paper presents a novel adhesive element that consists of two shell elements and one degenerated brick element. The element is formulated based on the assumption that only three out-of-plane strains, i.e., through-thickness normal and shear strains, are non-zero and constant across the adhesive layer. In this formulation, the adhesive thickness is assumed to be non-uniform. Illustrative numerical examples are presented to investigate the effect of non-uniform adhesive thickness on stress distributions of non-uniformly bonded and curved joints.

KEYWORDS: Bonded joints, curvature, non-uniform bondline thickness, stress, adhesive element.

INTRODUCTION

Adhesive bonding has been widely used as an effective technique to join structural components, in which applied load is transferred via the adhesive layer from one structural member to another one. When applying this technique to practical problems, one needs to consider many aspects, such as stress analysis, static and fatigue strength, surface preparation, selection of adhesives, durability, etc. One important aspect in the design of a bonded joint is an accurate tool of predicting stresses, stress intensity factors and failure strength. There exists a large amount of information on stress analysis of the bonded joints in the literature, and most of the currently available analysis methods for bonded joint designs are limited to flat plate geometries [1]. However, in addition to flat panels, curved panels or shell-type structures are often used in the design of metallic and composite structures, especially in aircraft and aerospace structures, such as fuselage and wing skins. Comparing to the knowledge of bonded joints to flat panels, current knowledge on the effect of curvature(s) on the performance and durability of bonded joints is extremely limited. This paper aims to develop an accurate and simple tool for determining stresses in adhesive layer.

Stresses in adhesive layer can be determined following two types of solution procedures, namely, analytical and numerical analysis procedures. In the analytical procedure, closed-form solutions for stresses may be obtained via introducing a number of assumptions, while in the numerical analysis procedure, finite element method is frequently used. In general, analytical solutions are limited to simple geometrical configurations and material properties, while finite element method is more versatile in terms of geometrical configuration and material properties. In finite element analysis, it is desirable to conduct a full 3-D analysis to obtain accurate and detailed stress information. Because a full 3-D analysis involves detailed modeling of the adhesive layer, structural components using brick elements and adequately fine mesh, it can be very expensive and may even become impossible under certain circumstances. Thus it is necessary to develop a simple, efficient and cost-effective finite element analysis procedure using simple adhesive elements to capture the main features of stresses in the adhesive layer, which enables an engineer to conduct a reliable rapid design of bonded joints. There are only a few literature available reporting development of adhesive elements for modeling adhesive between two flat substrates. Carpenter [2] developed two adhesive elements in which both shear and peel stresses are included in the finite element

* email: ltong@aero.usyd.edu.au Fax: +61-2-93514841 Phone: +61-2-93516949

formulation of the adhesive element. Kuo [3] modeled the adhesive layer by a number of shear springs and proposed a two-dimensional continuous shear spring element. However, the through-thickness normal stress, usually referred to as peel stress, in the adhesive layer was not included in the element formulation. Sun et al [4] presented an efficient model for bonded repair to cracked aluminum plates. In their model, both aluminum plate and composite patch are modeled separately by the Midlin plate element, whereas the adhesive layer is modeled with effective springs connecting the patch and aluminum plate. Tong and Sun [5] proposed a simple, efficient and cost-effective finite element formulation for adhesive elements, which can be used to investigate the effect of curvature on the stresses in the adhesive layer. However, in the finite element formulation, the adhesive thickness is assumed to be constant. In practical structures, an adhesive layer in a bonded joint is often non-uniform due to primarily lack of technologies for accurate control of bondline thickness in manufacturing process, especially for a curved joint. The effect of non-uniform adhesive layer thickness on stress in bonded joint is still unknown. In this paper, a novel finite element formulation is developed for adhesive elements for investigating stresses in bonded and curved joints with non-uniform adhesive thickness. Numerical results are presented to illustrate the effects of non-uniform adhesive thickness on stresses in adhesive layer.

FUNDAMENTAL FORMULATION OF ADHESIVE ELEMENT

To model the behavior of an adhesive layer in a structural joint, the following assumptions are adopted:

(a) Both adherends or structural components are perfectly bonded together;
(b) The adhesive layer is thin and flexible, and the three in-plane stresses in the adhesive are very small compared to the three out-of-plane stresses and they can be neglected. Similar to Tong and Sun [5], only the three out-of-plane stresses, i.e., normal or peel stress σ_{zz} and the two out-of-plane shear stresses τ_{yz} and τ_{xz}, are taken into account in the energy formulation of the adhesive layer; and
(c) The three out-of-plane stresses are assumed to be constant across the adhesive thickness;
(d) The two adherends are thin-walled structural components and can be modeled by employing the first-order shell theory.

The above assumptions can be used to develop the 16-node adhesive shell element as depicted in Figure 1. The element consists of two 8-node shell elements, modeling the two thin-walled adherends, and one pseudo brick element modeling the adhesive layer. Unlike the element presented by Tong and Sun [5], in this element the brick element sandwiched between the two shell elements is formulated to enable modeling of non-uniform adhesive layer.

As shown in Figure 1, all the nodes of each shell element are located on its mid-surface and are denoted by solid circle marks. The pseudo nodes of the 16-node adhesive element are marked as hollow circles and placed at the adhesive-shell interfaces, i.e., the upper surface of the lower shell element and the lower surfaces of the upper shell element. For convenience, we use subscript "$_1$" and "$_2$" to indicate the variable of upper and lower shell element, respectively. Let h_1 and h_2 denote the thickness of the upper and lower shell element respectively, which are constants, and t the thickness of the adhesive layer. Note that t is not constant and is dependent on location.

Two nodal coordinate systems and one local coordinate system, namely $x_1y_1z_1$, $x_2y_2z_2$ and $x'y'z'$, are employed to describe the nodal displacements and element strains. The nodal coordinate systems of $x_1y_1z_1$ and $x_2y_2z_2$ are the same as those defined in the shell element, which can be different from node to node. The subscript "$_1$" and "$_2$" represents that the shell, where the nodal coordinate system is constructed. The nodal displacements in this analysis are defined

in the nodal coordinate system. For the local coordinate system, z' is the outward normal of the mid-plane of the adhesive layer. x' and y' are tangent to the mid-plane of the adhesive layer. As shown in Fig.1, all the node pair of the brick element, such as 1-9, 2-10, etc., should be located in the outward normal z'. In other words, the line going through every node pair should coincide with the outward normal of the mid-plane of the adhesive layer. It should be noted that the three coordinate systems could be degenerated to a single nodal coordinate system if the thickness of the adhesive layer is constant.

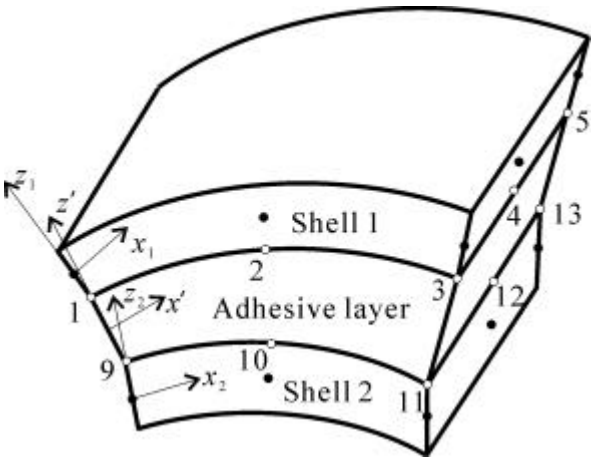

Fig. 1 A 16-node adhesive shell element allowing non-uniform thickness of the adhesive layer

Based on the basic assumption mentioned above, we can define three out-of-plane strains in the adhesive layer as follows

$$\begin{aligned} \boldsymbol{e}_{z'z'} &= \frac{w'_{1B} - w'_{2T}}{t} \\ \boldsymbol{g}_{z'x'} &= \frac{u'_{1B} - u'_{2T}}{t} \\ \boldsymbol{g}_{z'y'} &= \frac{v'_{1B} - v'_{2T}}{t} \end{aligned} \tag{1}$$

where the subscript "$_{1B}$" represents the bottom surface of the upper shell element, and "$_{2T}$" is the top surface of the lower shell element. The prime denotes that the displacements in equation (1) are defined in the local coordinate system. Moreover, the two locations of the upper and lower shell element, where the displacements are referred to, should be located in the same outward normal of the mid-plane of adhesive layer. The thickness t is the distance between two locations.

According to the first order shell theory that takes into account of transverse shear deformations, the displacements on the surface of the shell element can also be given by the corresponding displacements on the mid-plane, which are

$$\begin{aligned} w &= w^0 \\ u &= u^0 + z\boldsymbol{q}_y \\ v &= v^0 - z\boldsymbol{q}_x \end{aligned} \tag{2}$$

where the superscript "^{0}" denotes the mid-plane of the shell element. z is the distance from the mid-plane of shell element to the plane where the displacements are evaluated.

In general, for a shell element, the nodal displacements are defined in the nodal coordinate system as defined above. To establish the relationship between the strains and the nodal displacements, all these displacements must be transformed into one coordinate system. In this paper, the local coordinate system $x'y'z'$, which is constructed on the point that three strains in the adhesive layer are evaluated, is employed to evaluate three out-of-plane strains in the adhesive layer.

For the upper shell element, we can write the nodal displacement vector in its corresponding nodal coordinate system as

$$\begin{aligned} \{q_1\} &= \{q_{11} \quad \Lambda \quad q_{1i} \quad \Lambda \quad q_{18}\} \\ \{q_{1i}\} &= \{u_{1i}^0 \quad v_{1i}^0 \quad w_{1i} \quad \boldsymbol{q}_{xi} \quad \boldsymbol{q}_{yi}\} \qquad (i = 1,2,\Lambda\ ,8) \end{aligned} \tag{3}$$

Then the nodal displacement vector in the nodal coordinate system can be transformed into the local coordinate system

$$\{q'_{1i}\} = [T_{1i}]\{q_{1i}\} \tag{4}$$

where $[T_{1i}]$ is the transformation matrix of 5 5 between the local coordinate system and the nodal coordinate system of node *i* in the upper shell element.

The displacement field of shell element can be expressed by the nodal displacement as

$$\{q'_1\} = \sum_{i=1}^{8} [N_{1i}]\{q'_{1i}\} \tag{5}$$

where $[N_{1i}]$ is the shape function matrix of 8-node isoparametric element and has the form

$$[N_{1i}] = \begin{bmatrix} N_i & & & & & & & 0 \\ & N_i & & & & & & \\ & & N_i & & & & & \\ & & & N_i & & & & \\ 0 & & & & & & & N_i \end{bmatrix} \tag{6}$$

Then the displacement vector in the local coordinate system can be expressed as

$$\{q'_1\} = [\overline{N}_1][T_1]\{q_1\} \tag{7}$$

where

$$[T_1] = \begin{bmatrix} T_{11} & & & & & & & 0 \\ & \text{O} & & & & & & \\ & & T_{1i} & & & & & \\ & & & \text{O} & & & & \\ 0 & & & & & & & T_{18} \end{bmatrix} \qquad [\overline{N}_1] = [N_{11} \quad \Lambda \quad N_{1i} \quad \Lambda \quad N_{18}] \tag{8}$$

Similarly, the nodal displacement vector in the local coordinate system for the lower shell element can be written as

$$\{q'_2\} = [\overline{N}_2][T_2]\{q_2\} \tag{9}$$

where $\{q'_2\}$, $[\overline{N}_2]$, $[T_2]$ and $\{q_2\}$ can be defined by replacing the upper shell subscript "$_1$" with the lower shell subscript "$_2$" in equations (3)-(8).

Substitute equation (2) and equation (7), (9) into equation (1) and write in matrix form, we can obtain

$$\begin{Bmatrix} e_{z'z'} \\ g_{z'y'} \\ g_{z'x'} \end{Bmatrix} = \frac{1}{t}\begin{bmatrix} 0 & 0 & 1 & 0 & 0 & 0 & 0 & -1 & 0 & 0 \\ 0 & 1 & 0 & \frac{h_1}{2} & 0 & 0 & -1 & 0 & \frac{h_2}{2} & 0 \\ 1 & 0 & 0 & 0 & -\frac{h_1}{2} & -1 & 0 & 0 & 0 & -\frac{h_2}{2} \end{bmatrix} [\overline{N}][T] \begin{Bmatrix} q_1 \\ q_2 \end{Bmatrix} \tag{10}$$

where

$$[\overline{N}] = \begin{bmatrix} \overline{N}_1 & 0 \\ 0 & \overline{N}_2 \end{bmatrix}, \qquad [T] = \begin{bmatrix} T_1 & 0 \\ 0 & T_2 \end{bmatrix} \tag{11}$$

Then we can obtain the geometric matrix for the adhesive layer

$$[B] = \frac{1}{t}\begin{bmatrix} 0 & 0 & 1 & 0 & 0 & 0 & 0 & -1 & 0 & 0 \\ 0 & 1 & 0 & \frac{h_1}{2} & 0 & 0 & -1 & 0 & \frac{h_2}{2} & 0 \\ 1 & 0 & 0 & 0 & -\frac{h_1}{2} & -1 & 0 & 0 & 0 & -\frac{h_2}{2} \end{bmatrix} [\overline{N}][T] \tag{12}$$

The elastic matrix for this pseudo brick element is

$$[D] = \begin{bmatrix} E & 0 & 0 \\ 0 & G & 0 \\ 0 & 0 & G \end{bmatrix} \tag{13}$$

where E is the Young's modulus and G is the shear modulus of adhesive layer.

Then the element stiffness matrix for the adhesive brick element can be given

$$[K] = \int_V [B]^T [D][B] dV \tag{14}$$

A numerical integration scheme, $2 \times 2 \times 1$ Gaussian quadrature, is employed to evaluate the stiffness matrix in equation (14). The thickness of the adhesive layer used in [B] should be that of the adhesive layer at the Gaussian point and the local coordinate system $x'y'z'$ should also be constructed on the Gaussian point. The stiffness matrix of the adhesive element can be subdivided into four sub-matrix, which can be assembled to the global stiffness matrix in the same way as detailed in Tong and Sun [5].

NUMERICAL EXAMPLES AND DISCUSSION

An externally reinforced patch is bonded to the cylindrical shell, as shown in Fig. 2. The circular cylindrical shell and patch are assumed to be metallic and has a Young's modulus of 70 GPa and a Poisson's ratio of 0.3. The adhesive has a Young's modulus of 2.4 GPa and a Poisson's ratio of 0.33. The geometric parameters are: L=150mm, arc length C=30mm, width of curved shell w=10mm, thickness of shell and patch H=5mm. The outer radius of the cylindrical shell is R and the inner radius of patch is r, respectively. There is an eccentricity e between the two circle centers of cylindrical shell and bonded patch.

According to the symmetry of the structure with the symmetric load selected, two elements are divided in y direction and 60 elements are used in the patch along the circular direction.

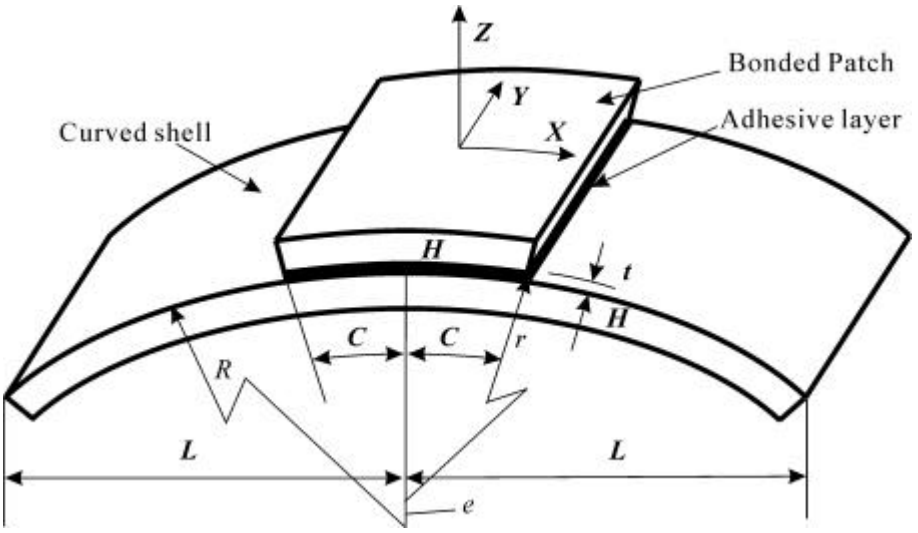

Fig. 2 A cracked cylindrical shell with an externally boned patch

(a) A curved shell with a bonded patch subjected to tensile load

The vertical displacements and rotation about y-axis at both ends of the circular cylindrical shells are assumed to be zero. A uniformly distributed load of 10 N/mm along the width of the circular cylindrical shell is applied upward at the middle point of shell. Four values of radius of cylindrical shell are considered, which are (1) R=150mm, (2) R=300mm, (3) R=450mm, (4) R=600mm. The thickness of the adhesive layer in the middle of the cylindrical shell is kept to be constant, which is t=0.15mm. For all the cases, three kinds of eccentricity, which are 0.0mm, -1.0mm, 1.0mm, are calculated. Both of peel and shear stresses distributions in the adhesive layer along half the adhesive bondline for R=150mm along y=±2.9mm are depicted in Fig. 3. For e=0.0mm, the adhesive element is degenerated to the former one proposed by Tong and Sun [5] and the same results are obtained using the two elements. From Fig.3, it can be seen that the stress distributions are similar for all three cases. But the peak stresses at the end of the adhesive layer (at the Gaussian point) have different values. The peak peel and shear stress values and their variation from that of uniform adhesive layer are given in Table 1. In the case of R=150mm, for the patch which has radius r=151.15mm, the thickness of the adhesive layer varies from 0.15mm to 0.17mm. The peak peel stresses are smaller than that of uniform adhesive. For r=149.15mm, the thickness of the adhesive layer varies from 0.15mm to 0.13mm. The peak peel stress is larger than that of uniform adhesive. For all three eccentricity cases, the peak shear stress is affected by the variation of the thickness of adhesive layer in the same form. The results for all values of R

indicate that variation in adhesive thickness tends to have a more remarkable effect on the peel stress than on the shear stress.

(b) A curved shell with a bonded patch subjected to internal pressure load

The boundary and the size of the structure are same as that in (a). The shell is subjected internal pressure load p=1.0Mpa. Both of the peel and shear stresses distributions in the adhesive layer for R=150mm are depicted in Fig. 4. The peak peel and shear stress values and their variation from that of uniform adhesive layer are given in Table 2 for different values of R=150, 300, 450 and 600mm. From Fig. 4 and Table 2, we can see that the peak stress becomes larger when the thickness of the adhesive layer decreases at the end of the patch, while it becomes smaller when the thickness of the adhesive layer increases. In this example, a bigger eccentricity e=±5.0mm is also considered. It is easy found that, for the same curvature, The peak values of stress at the end of adhesive layer increase with a decreased adhesive thickness and decrease with an increased adhesive thickness.

CONCLUDING REMARKS

In this paper, A novel adhesive element formulation is developed based on assumption that the three out-of-plane strains are constant across the adhesive layer thickness to analyze non-uniformly bonded and curved joint. The selected numerical examples demonstrate the following observations:

(a) The peel and shear stress peak at the end of the adhesive layer;
(b) The peak values increase with a decreased adhesive thickness and decrease with an increased adhesive thickness;
(c) The effect of adhesive thickness becomes more noticeable when coupled with large curvature;
(d) Peak peel stress seems to be more sensitive to varying adhesive thickness than the peak shear stress does.

ACKNOWLEDGEMENT

The project was supported by AOARD/AFOSR and ARC. The authors wish to thank Dr G. Schoeppner of AFRL and Dr T. Kim of AOARD/AFOSR for their valuable discussions and encouragement.

REFERENCES

1. Tong L and Steven G P, *Analysis and Design of Structural Bonded Joints*. Kluwer Academic Publishers: Boston; 1999
2. Carpenter C A., Stresses in bonded connections using finite elements, *International Journal for Numerical Methods in Engineering*, Vol.15 (1980), pp. 659-1680
3. Kuo A S, A two-dimensional shear spring element, *AIAA Journal*, Vol.22, No.10 (1984), pp.1460-1464
4. Sun CT, Klug J and Arendt C, Analysis of cracked aluminum plates repaired with bonded composite patches, *AIAA Journal*, Vol.34, No.2 (1996), pp.369-374
5. Tong L and Sun X., Stresses in bonded repair to cylindrically curved shell structures, FEARC-00-001, Contract Report, Department of Aeronautical Engineering, University of Sydney, NSW Australia, 2000

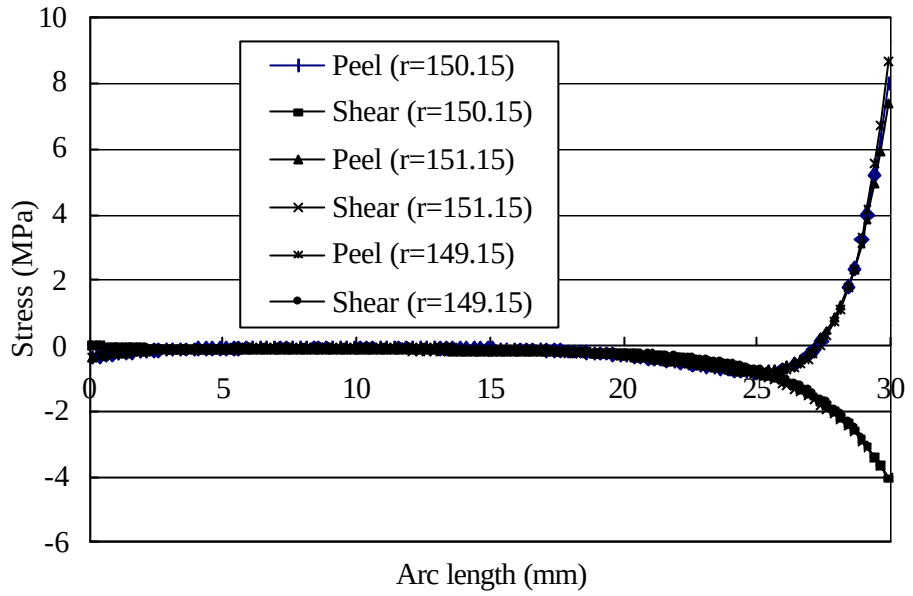

Fig. 3 Stress distribution in the adhesive layer for a curved shell with a bonded patch subjected to a tensile load (R=150 mm, y=±2.9mm)

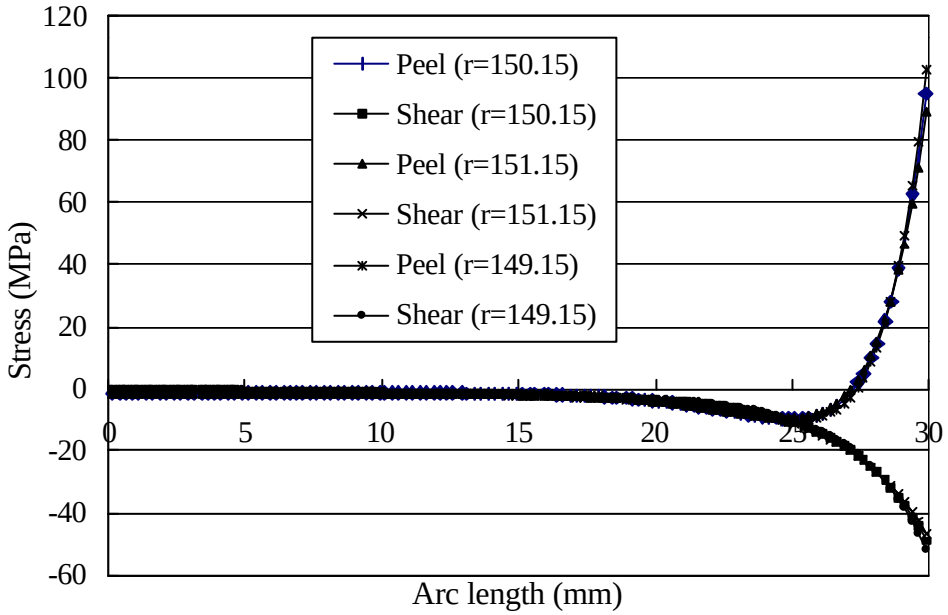

Fig. 4 Stress distribution in the adhesive layer for a curved shell with a bonded patch subjected to an internal pressure (R=150 mm, y=±2.9mm)

Table 1 Peak stress at the end of the adhesive layer (x=29.9mm) for a curved shell with a bonded patch subjected to a tensile load
(Values in the parentheses are variation from that of uniform adhesive layer)

Radius (mm)		Thickness at the end of the adhesive layer	Peak peel stress (MPa)	Peak shear stress (MPa)
R=150	*r*=150.15	0.15	8.00	-4.05
	r=151.15	0.17 (+13.3%)	7.41 (-7.4%)	-4.00 (-1.2%)
	r=149.15	0.13 (-13.3%)	8. 69 (+8.6%)	-4.10 (+1.2%)
R=300	*r*=300.15	0.15	1.74	-0.98
	r=301.15	0.155 (+3.3%)	1.71 (-1.7%)	-0.96 (-2.0%)
	r=299.15	0.145 (-3.3%)	1.77 (+1.7%)	-0.99 (+1.0%)
R=450	*r*=450.15	0.15	1.81	-1.07
	r=451.15	0.1522 (+1.5%)	1.80 (-0.6%)	-1.06 (-1.0%)
	r=449.15	0.1478 (-1.5%)	1.82 (+0.6%)	-1.08 (+1.0%)
R=600	*r*=600.15	0.15	1.96	-1.20
	r=601.15	0.15124 (+0.8%)	1.95 (-0.5%)	-1.20 (0.0%)
	r=599.15	0.14876 (-0.8%)	1.97 (+0.5%)	-1.21 (+1.0%)

Table 2 Peak stress at the end of the adhesive layer (x=29.9mm) for a curved shell with a bonded patch subjected to an internal pressure
(Values in the parentheses are variation from that of uniform adhesive layer)

Radius (mm)		Thickness at the end of the adhesive layer	Peak peel stress (MPa)	Peak shear stress (MPa)
R=150	*r*=150.15	0.15	95.3	-48.8
	r=151.15	0.17 (+13.3%)	89.2 (-6.4%)	-46.5 (-4.7%)
	r=149.15	0.13 (-13.3%)	103.0 (+7.3%)	-51.6 (+5.7%)
R=300	*r*=300.15	0.15	52.9	-29.5
	r=301.15	0.155 (+3.3%)	52.1 (-1.5%)	-29.0 (-1.7%)
	r=305.15	0.174 (+16.0%)	48.9 (-7.6%)	-27.4 (-7.2%)
	r=299.15	0.145 (-3.3%)	53.9 (+1.9%)	-30.0 (+1.7%)
	r=295.15	0.125 (-16.7%)	58.2(+10.0%)	-32.2 (+9.3%)
R=450	*r*=450.15	0.15	55.1	-32.3
	r=451.15	0.1522 (+1.5%)	54.7 (-0.7%)	-32.1 (-0.6%)
	r=449.15	0.1478 (-1.5%)	55.6 (+0.9%)	-32.6 (+0.9%)
R=600	*r*=600.15	0.15	59.7	-36.3
	r=601.15	0.15124 (+0.8%)	59.5 (-0.3%)	-36.1 (-0.6%)
	r=605.15	0. 15615 (+4.1%)	58.5 (-2.0%)	-35.6 (-1.9%)
	r=599.15	0. 14876 (-0.8%)	60.0 (+0.5%)	-36.4 (+0.3%)
	r=595.15	0.14375 (-4.2%)	61.1 (+2.3%)	-36.9 (+1.7%)